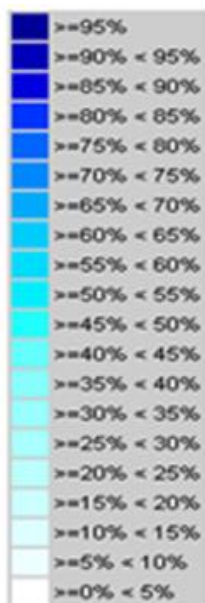


Supplemental data 1 A.



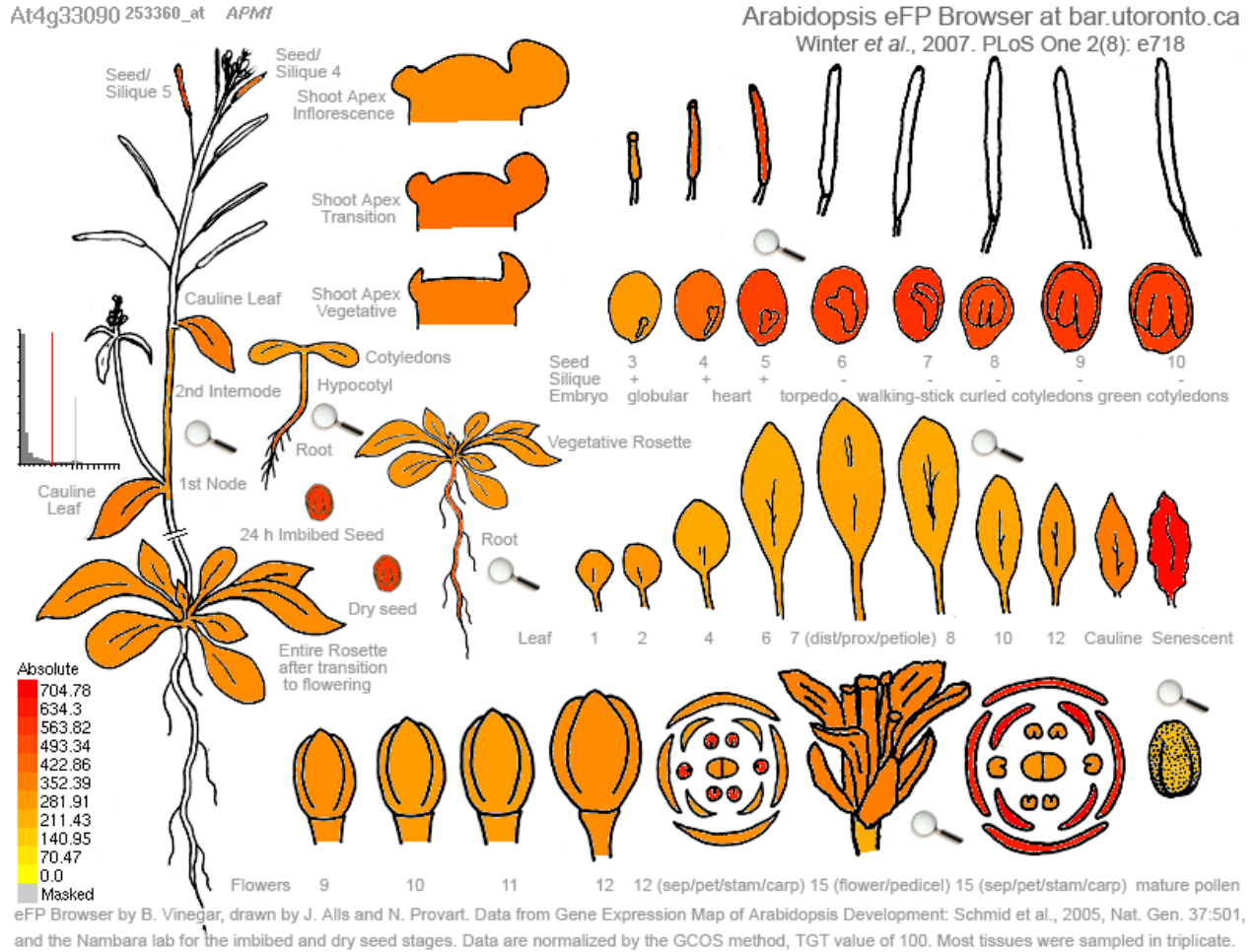
Development

Probeset											AGI/Links/Annotation
253360_at											AT4G3309

Organs

0 callus	
1 cell suspension	
2 seedling	
21 cotyledons	
22 hypocotyl	
23 radicle	
3 inflorescence	
31 flower	
311 carpel	
3111 ovary	
3112 stigma	
312 petal	
313 sepal	
314 stamen	
3141 pollen	
315 pedicel	
32 silique	
33 seed	
34 stem	
35 node	
36 shoot apex	
37 cauline leaf	
4 rosette	
41 juvenile leaf	
42 adult leaf	
43 petiole	
44 senescent leaf	
45 hypocotyl	
451 xylem	
452 cork	
5 roots	
52 lateral root	
53 root tip	
54 elongation zone	
55 root hair zone	
56 endodermis	
57 endodermis+cortex	
58 epid. trichoblasts	
59 lateral root cap	
60 stele	

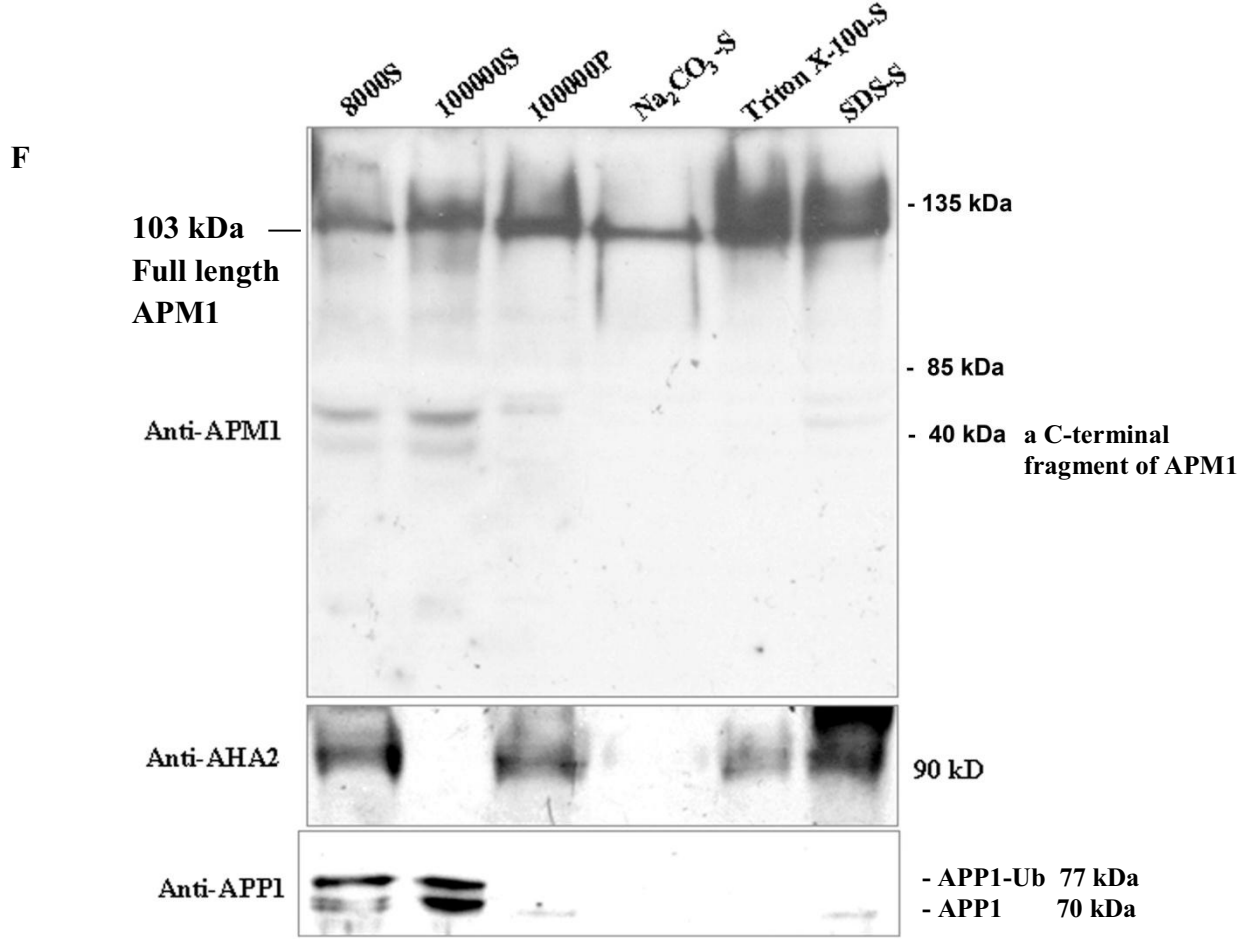
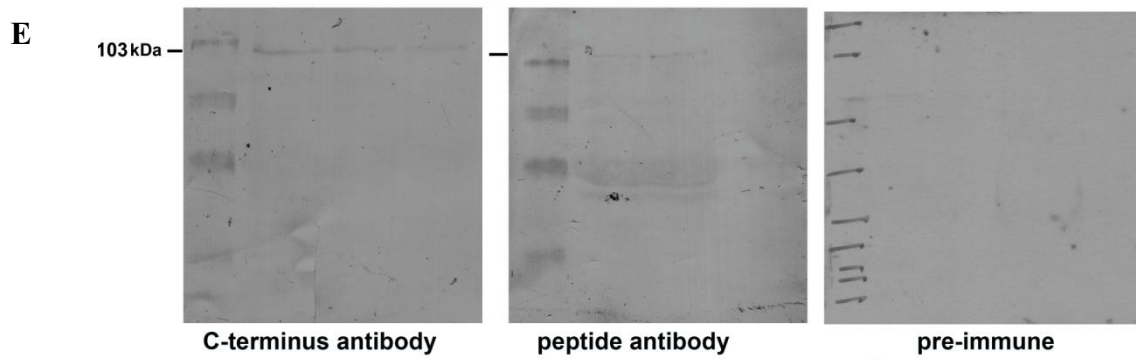
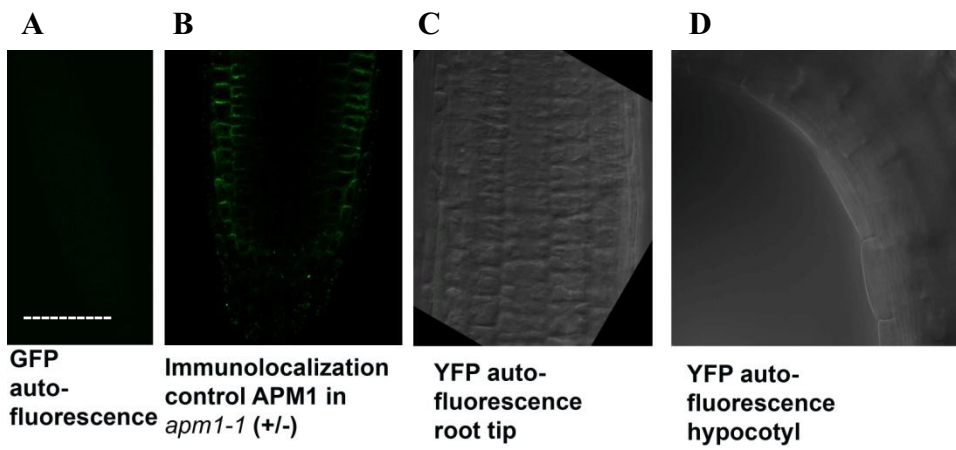
Supplemental data 1 B.



Supplemental data 1. *APM1* expression from microarrays. The sequence used by Affymetrix to generate the *APM1* hybridization sequences on the current Arabidopsis expression chip includes one oligonucleotide sequence from an intron in the *APM1* gene resulting in poor representation of *APM1*.

Supplemental data 1A. Genvestigator (Zimmerman et al., 2004) microarray analysis of expression patterns of *APM1*.

Supplemental data 1B. Arabidopsis eFP browser (Winter et al., 2007).microarray analysis of expression patterns of *APM1*.



Supplemental data 2. Controls for autofluorescence, immunolocalization, western blot and analysis of APM1 topology.

Autofluorescence controls

(A) GFP autofluorescence of an embryo is shown taken with the same setting used for all *ProAPM1*:GFP data. GFP autofluorescence of a root is also shown in Figure 1N taken with the same setting used for all *ProAPM1*:GFP data.

(B) Immunolocalization control of APM1 antibody in *apm1-1* (+/-) seedling. Faint signal can be observed in the epidermis, as might be expected since there are no knockout alleles. The signal in a wild type seedling is much stronger (Figure 11A). These images were taken with the same settings.

(C), (D) Images of 5-d-old wild-type root and hypocotyl were taken with the same settings used for *ProAPM1*:YFP-APM1 images in the main body of the manuscript. No signal is observed in the wild type.

Size bar in A: A, B, 50 μm ; C, D 20 μm .

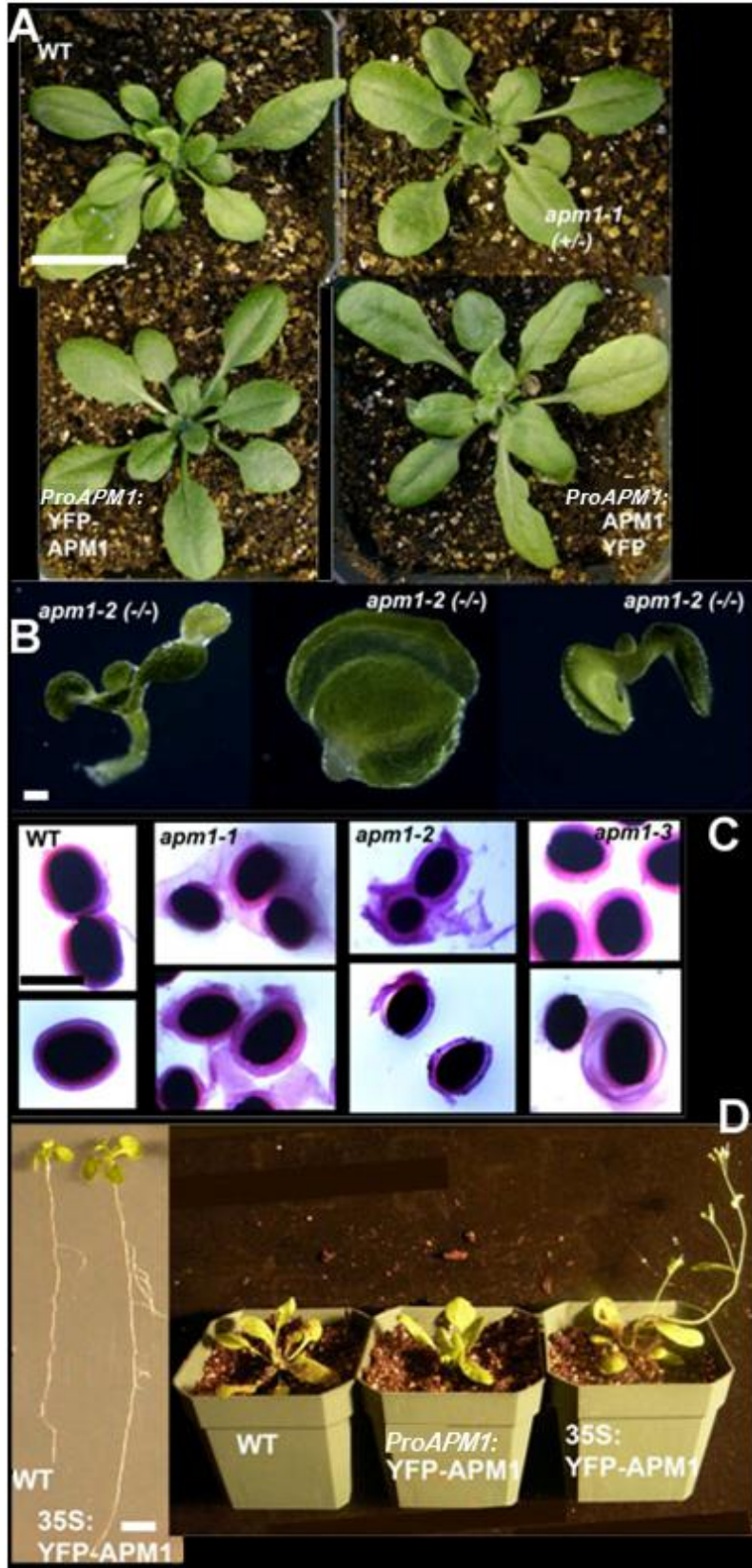
Antibody western blots

(E) 103 kDa bands are observed in western blots using the C-terminus or peptide anti-APM1 antisera. No signal at 103 kDa is observed in the pre-immune western blot. Lanes are a dilution series of 5-d-old Arabidopsis microsomal membrane preparation.

APM1 topology

(F) In order to verify the mixed membrane and cytosolic association of APM1, microsomal membranes were prepared from 5-d-old Arabidopsis seedlings, differentially solubilized, and analyzed by western blot analysis with the APM1 peptide antiserum. As was seen previously with the C-terminal APM1 antisera (Murphy et al., 2002), full-length APM1 (103 kDa) and a 42 kDa APM1 C-terminal degradation product [previously described and sequenced in Murphy et al. (2002) as APM1 Δ , and sequenced again here] were detected in the 8,000 g and 100,000 g supernatants and 100,000 g pellets, although only a small amount of the degradation product was present in the 100,000 g pellet (42 kDa). The antibody is to the C-terminus of APM1; therefore this product is recognized by the antibody. This C-terminal deletion product is only seen during

microsomal preparation, and may be due to autocatalysis of APM1 or other catalytic activity. We re-sequenced this band to verify it. Consistent with APM1 being associated with the membrane, full-length APM1 (103 kDa) could be released from the 100,000 g microsomes with 0.1 M Na_2CO_3 , while Triton X-100 and SDS pretreatment enhanced release of APM1 from the 100,000 g pellet compared to SDS sample buffer alone. In contrast, the plasma membrane marker AHA2 could only be displaced from membranes by Triton X-100 and SDS pretreatment, while a soluble protein, APP1, was only found in soluble fractions, and its localization was not altered by pretreatments (Supplemental data 2 F). These results indicate that APM1 is a peripheral membrane (rather than type II membrane anchored) protein and that a sub-population of APM1 is more easily displaced from membranes.



Supplemental data 3. Complementation and mutant phenotypes.

(A) *apm1-1* mutants were complemented with Pro*APM1*:YFP-APM1 or Pro*APM1*: APM1-YFP and are shown at 5 weeks after germination.

(B) Additional images of *apm1-2* seedlings.

(C) Rhuthenium red staining of mucilage from imbibed seeds show a more diffuse radius and web-like mucilage of *apm1* mutants compared to the wild type.

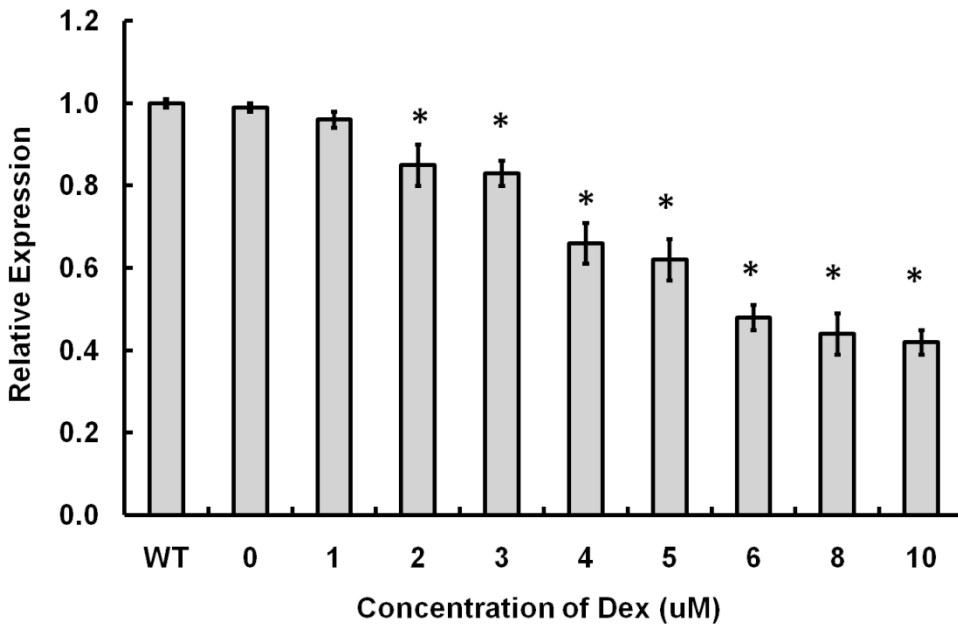
(D) Wild type (WT) plants and *apm1-1* plants transformed with Pro35*S*:YFP-APM1 are shown. Pro35*S*:YFP-APM1 seedlings develop lateral roots sooner than wild type seedlings, 10 day seedlings are shown.

35*S*pro:YFP-APM1 plants develop faster than wild type and Pro*APM1*:YFP-APM1 plants, 24-day-old plants are shown.

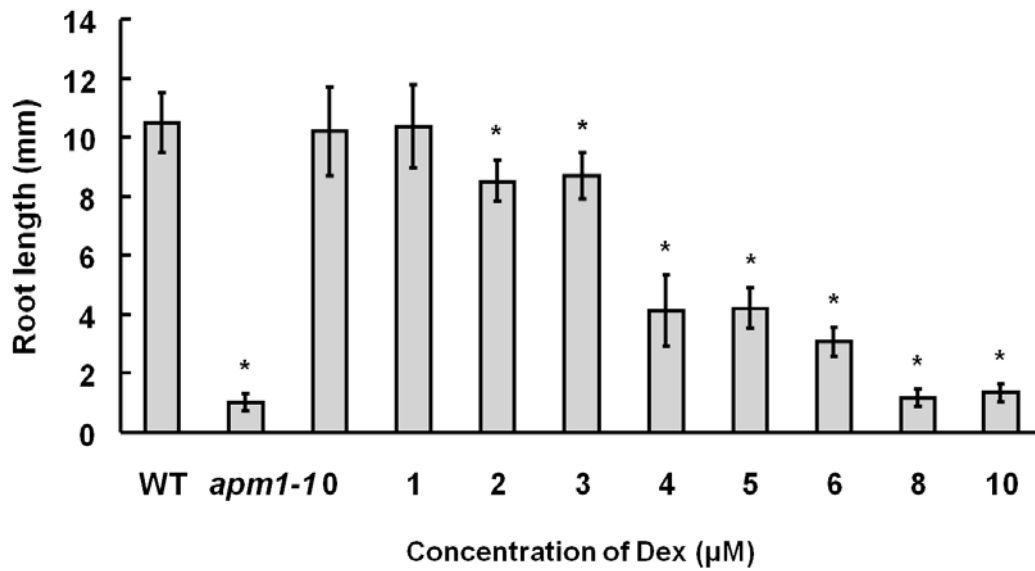
Size bars, A, 2 cm; B, 200 μ m; C, 250 μ m; D, 1 cm.

Supplemental data 4.

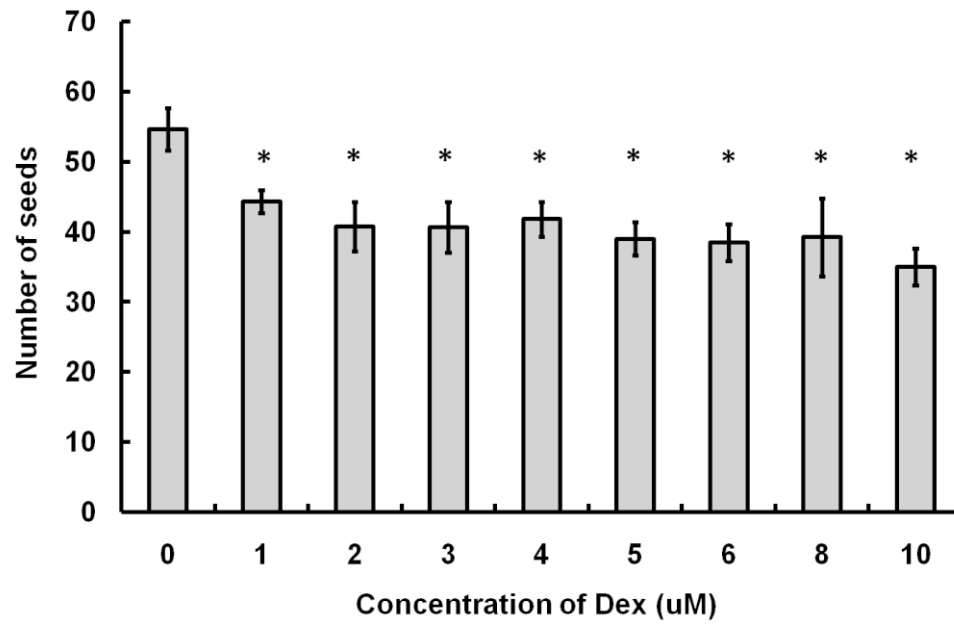
A. QRT-PCR pOpOff



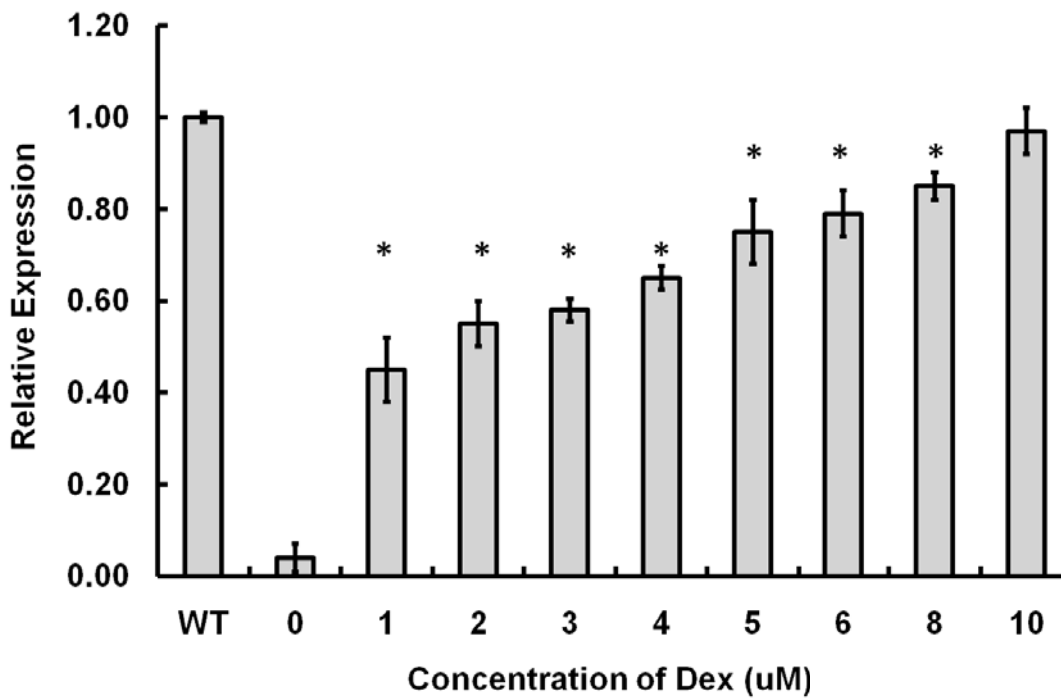
B. Root length quantitation pOpOff



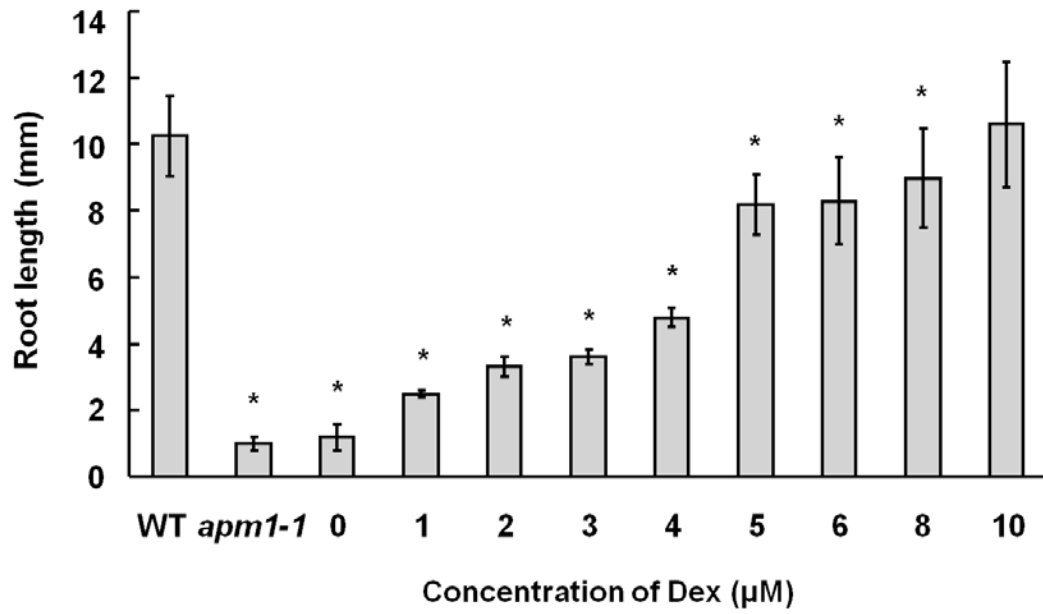
C. Seed quantitation pOpOff



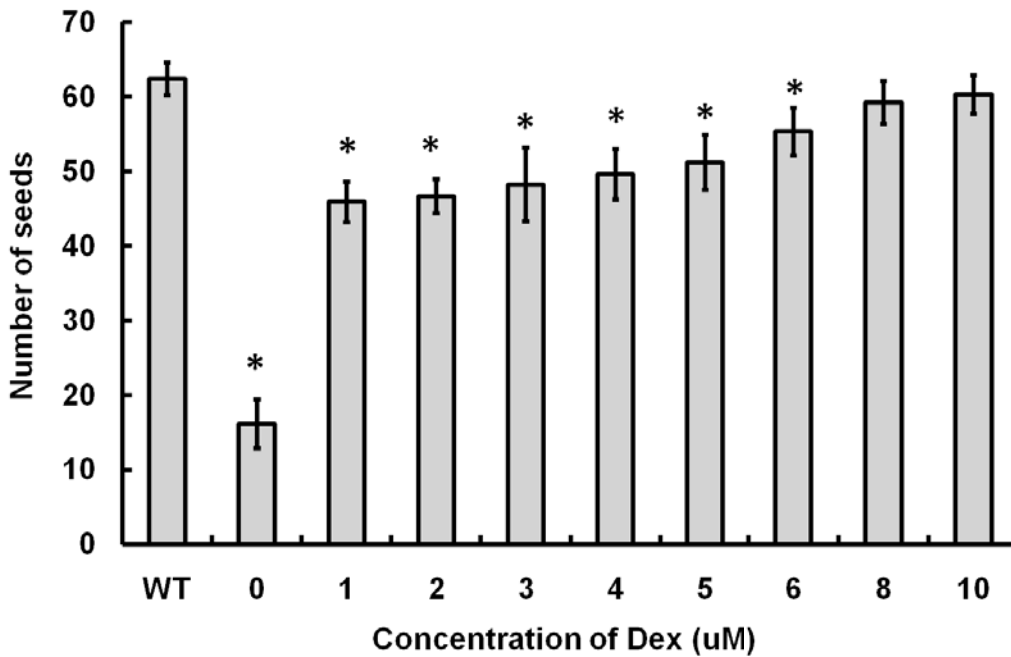
D. QRT-PCR pOpOn



E. Root length quantitation pOpOn



F. Seed quantitation pOpOn



Supplemental data 4. Quantitative real-time PCR analysis of inducible silencing and induction of *APM1* expression, quantitation of seed data.

(A) Quantitative real-time PCR analysis of wild-type plants transformed with pOpOff, induced with indicated concentrations of dexamethasone (Dex) to silence *APMI* expression. Data are means and standard deviations from three independent experiments. * $P < 0.05$ compared to wild type; ANOVA followed Tukey's post-hoc analysis.

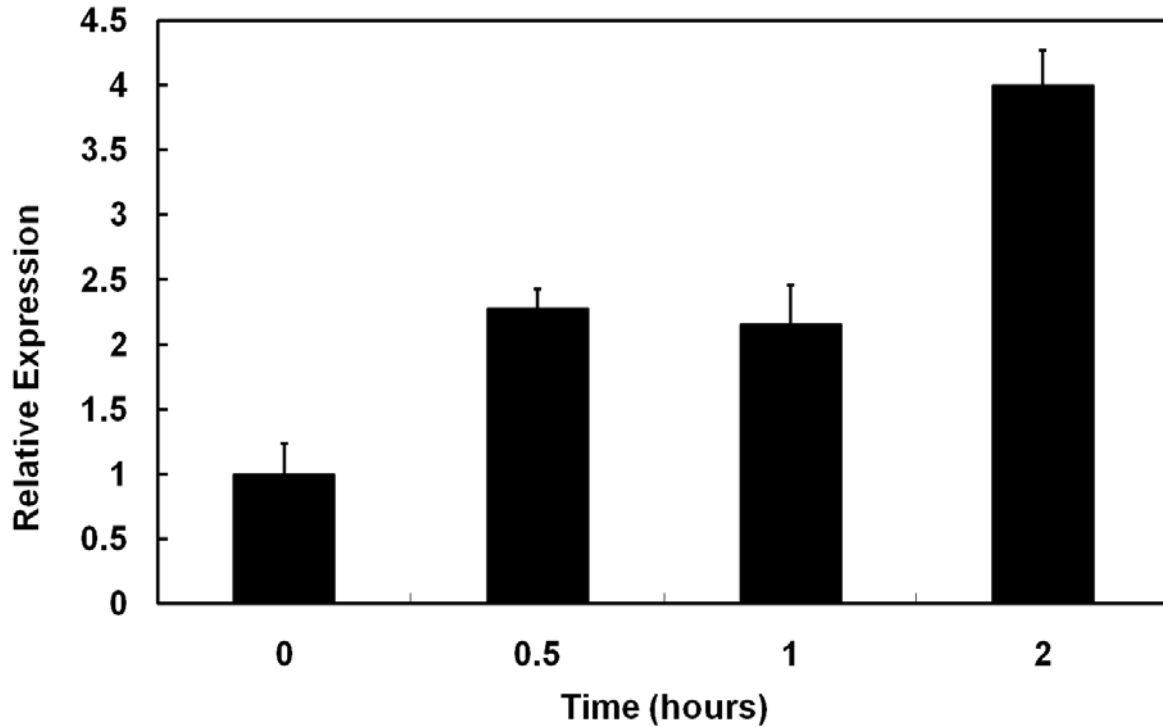
(B) Quantification of root length from wild-type plants carrying pOpOFF. *APMI* expression was silenced with indicated Dex concentrations. Root lengths of resultant seedlings were quantified. Data are means and standard deviations from three independent experiments, $n=20$. * $P < 0.001$ compared to wild type, ANOVA followed Tukey's post-hoc analysis.

(C) Quantification of seeds from wild-type plants carrying pOpOFF. *APMI* expression was silenced with indicated Dex concentrations. Resultant siliques were harvested and seeds quantified. Data are means and standard deviations, $n=10$. * $P < 0.001$ compared to wild type, ANOVA followed Tukey's post-hoc analysis.

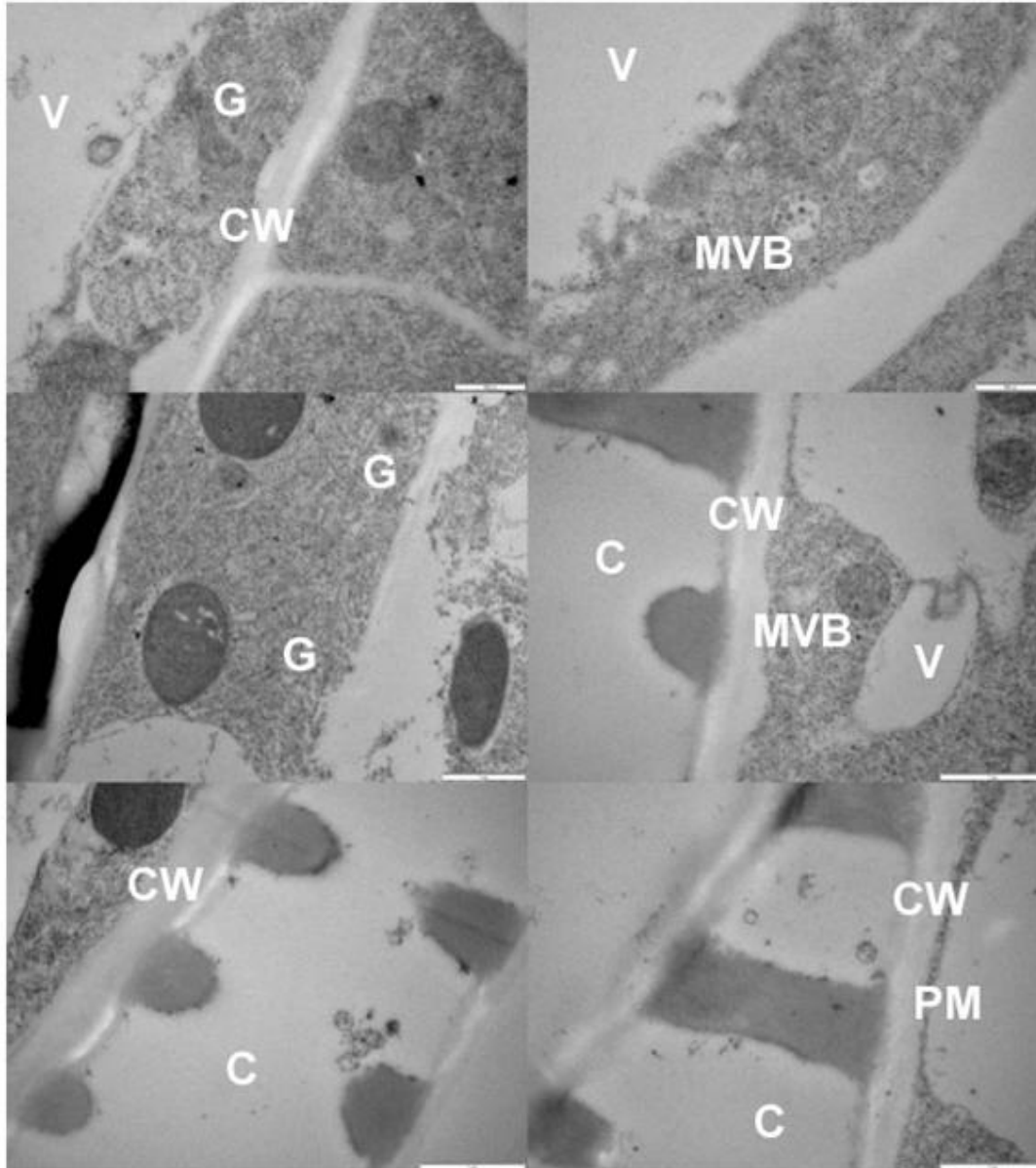
(D) Quantitative real-time PCR analysis of *apm 1-1* plants transformed with pOpON YFP-APM1. *APMI* expression was induced with indicated Dex concentrations. Data are means and standard deviations from three independent experiments. * $P < 0.05$ compared to wild type; ANOVA followed Tukey's post-hoc analysis.

(E) Quantification of root length of *apm 1-1* plants transformed with pOpON YFP-APM1. *APMI* expression was induced with indicated Dex concentrations. Root lengths of resultant seedlings were quantified. Data are means and standard deviations from three independent experiments, $n=20$ * $P < 0.05$ compared to wild type; ANOVA followed Tukey's post-hoc analysis.

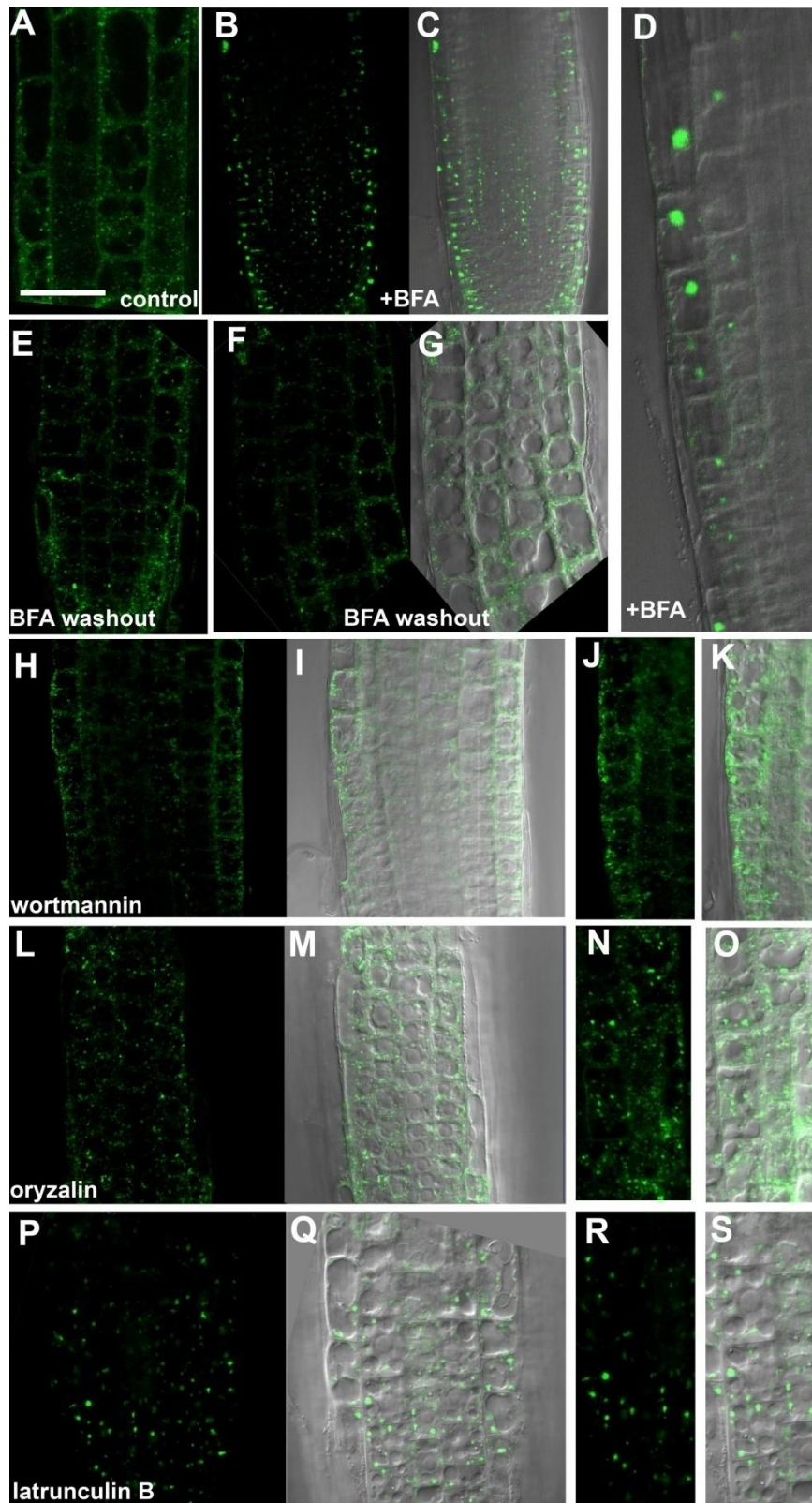
(F) Quantification of seeds from *apm 1-1* plants carrying pOpON YFP-APM1. *APMI* expression was induced with indicated Dex concentrations and resultant siliques were harvested and seeds quantified. Data are means and standard deviations, $n=10$. * $P < 0.001$ compared to wild type, ANOVA followed Tukey's post-hoc analysis.



Supplemental data 5. Quantitative real-time PCR analysis of *APM1* expression after IAA treatment. Quantitative real-time PCR analysis of *APM1* expression in 5-d-old wild-type seedlings after treatment with 1 μ M IAA. The expression pattern appears to be two-staged, consisting of an initial primary response (30 min), and a secondary response (2 h). Data are means and standard deviations from three independent experiments.



Supplemental data 6. Electron micrographs of pre-immune controls for APM1 antibodies. C, cytosol, CW, cell wall, G, Golgi, MVB, multi-vesicular body, PM, plasma membrane. Size bars, top panel 500 nm, middle and bottom panels, 1 μ m.



Supplemental data 7. APM1 localization is affected by trafficking inhibitors.

5d Pro*APM1*:YFP-APM1 seedlings were examined.

(A) Untreated Pro*APMI*:YFP-APM1 seedling root tip.

(B)-(G) Seedling root tips treated with 5 μ M brefeldin A (BFA) for 30 min **(B)** Aggregations of Pro*APMI*:YFP-APM1 signal are observed **(C)** DIC overlay of B. **(D)** Detail of APM1 localization in epidermal cells and cortical cells following BFA treatment. **(E)** The seedlings were examined 2 h after BFA washout. Pro*APMI*:YFP-APM1 localization was almost completely restored. **(F)** Detail of E. **(G)** DIC overlay of F.

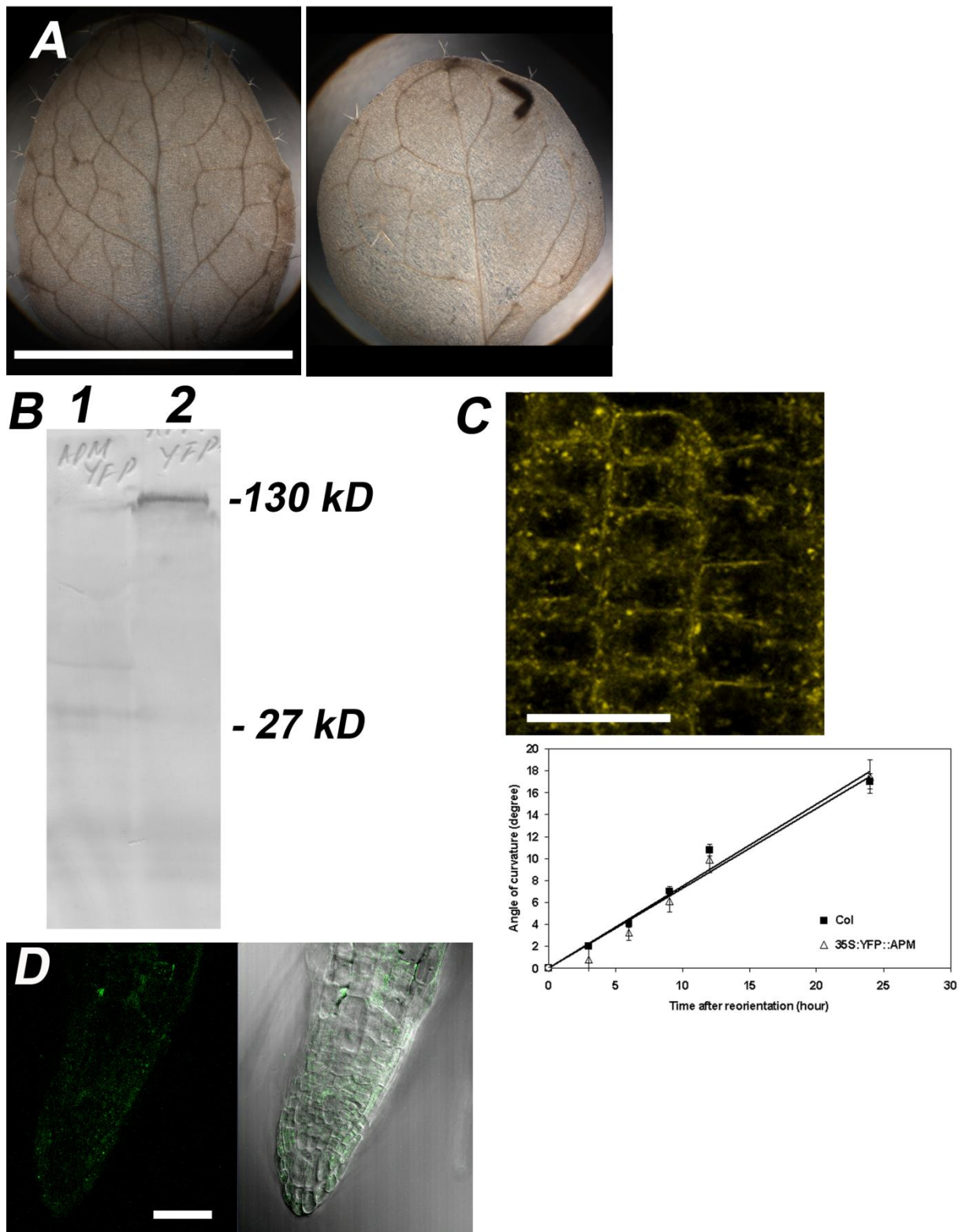
(H)-(I) Treated with 33 μ M wortmannin for 60 min. **(H)** Some aggregation of Pro*APMI*:YFP-APM1 was observed in the epidermal cells files. **(I)** DIC overlay of H. **(J)** Detail of H. **(K)** DIC overlay of J.

(L)-(O) Treated with 10 μ M oryzalin for 60 min. **(L)** Pro*APMI*:YFP-APM1 localization was not affected. **(M)** DIC overlay of L. **(N)** Detail of L. **(O)** DIC overlay of N.

(P)-(S) Treated with 10 μ M latrunculin B for 60 min. **(P)** Aggregation of the Pro*APMI*:YFP-APM1 signal was observed. **(Q)** DIC overlay of P. **(R)** Detail of P. **(S)** DIC overlay of R.

~30 seedlings per experiment; experiments were repeated twice; the results presented were observed in >90% of the seedlings.

Size bar in A: A, E, F, G, 25 μ m; B, C, L, M, 50 μ m; D, J, K, N, O, R, S, 10 μ m; H, I, P, Q, 30 μ m.



Supplemental data 8. Leaf phenotypes, western blot of YFP C-terminal fusions, additional 35S overexpression data, and *SCR* expression in *apm1-1* (-/-).

(A) Leaf from wild-type plant (left) and leaf from *apm1-1* (+/-) plant (right). *apm1-1* has fewer vascular traces than wild type.

(B) Western blot of Arabidopsis microsomal membranes of *apm1-1* plants transformed with YFP fusions to APM1 and probed with anti-YFP. APM1 is ~103 kD and YFP is ~27 kD, therefore the protein fusion should be ~130 kD. Lane 1, Pro*APMI*:APM1-YFP. Lane 2, Pro*APMI*:YFP-APM1. The YFP is cleaved from the APM1-YFP C-terminal fusion (Pro*APMI*:APM1-YFP), but the expected size for the N-terminal YFP-APM1 (Pro*APMI*:YFP-APM) has the predicted molecular weight.

(C) Confocal image of Pro35*S*:YFP-APM1 signal in *apm1-1*. Although Pro35*S*:YFP-APM1 plants have more YFP signal and develop faster than wild-type plants, gravitropism was unaltered compared to wild type.

(D) Ectopic expression of Pro*SCR*:GFP in *apm1-1* (-/-) in epidermal cells.

Size bar: A, 3 cm; C, 20 μ m; D, 50 μ m.

References

Winter, D., Vinegar, B., Nahal, H., Ammar, R., Wilson, G.V., and Provart, N.J. (2007). An "electronic fluorescent pictograph" browser for exploring and analyzing large-scale biological data sets. *PLoS ONE* **2**: e718.

Zimmermann P, Hirsch-Hoffmann M, Hennig L, Gruissem W (2004) GENEVESTIGATOR. Arabidopsis Microarray Database and Analysis Toolbox. *Plant Physiol* **136**: 2621-2632.